

**ROTARY-BALANCE TEST COMPARISONS WITH
AGARD WG-16 GENERIC FIGHTER MODEL**

by

G. N. Malcolm, B. R. Kramer and C. J. Suárez
Eidetics International, Inc.
Torrance, CA

C. O. O'Leary, B. Wier, and J. M. Walker
Defence Research Agency
Bedford, UK

L. Visintini
AerMacchi S.p.A.
Venegono, Italy

F. Rafatnia and L. Fernkrans
Aeronautical Research Institute of Sweden
Bromma, Sweden

Abstract

AGARD Working Group 16 is performing a "Cooperative Program on Rotary Experiments for Maneuvering Aircraft Dynamics" focused on rotary-balance and forced-oscillation tests at high angles of attack in many different wind tunnels on identical models of a sharp ogive-nose generic fighter configuration. The goals are to compare results and evaluate wind tunnel wall and model support interference effects, correlate rotary-balance and forced-oscillation results, evaluate configuration build-up effects, understand the physics of rotary flows and their effects on the forces and moments, and to provide a data base for aerodynamic math modeling studies and for comparison and validation of computational aerodynamic methods. In general, good agreement was found between various facilities for configurations with forebody strakes. More variation in the lateral-directional characteristics was observed for configurations without forebody strakes. Reynolds number effects are less significant for configurations with strakes, which help stabilize or fix the flow separation on the nose. Comparisons for different model sizes in the same tunnel or with the same model with an open and closed test section also show insignificant differences. Effects of different sting mounting arrangements in the same tunnel show, in some cases, very large differences for the model without strakes and minor differences with strakes.

Nomenclature

a, α Angle of attack (AOA)
b Wing span, (A) 2.250 ft, 0.6862 m
(B) 1.643 ft, 0.501 m

\bar{c} Wing mean aerodynamic cord,
(A) 1.039 ft, 0.3168 m
(B) 0.758 ft, 0.2313 m
cm Center of moments (rotation center),
from base (0.276 \bar{c})
(A) 1.400 ft, 0.427 m
(B) 1.008 ft, 0.3072 m
 C_l (CLB) Rolling moment coefficient (body axis)
 C_N (CN) Normal force coefficient (body axis)
 C_n (CNB) Yawing moment coefficient (body axis)
 C_y (CY) Side force coefficient (body axis)
d Diameter of fuselage,
(A) 0.328 ft, 0.100 m
(B) 0.2394 ft, 0.073 m
q Dynamic pressure, $1/2 \rho V^2$
R Reynolds number based on \bar{c}
 R_d Reynolds number based on d
S Wing reference area,
(A) 2.0828 ft², 0.1936 m²
(B) 1.1103 ft², 0.1032 m²
V Free stream velocity
 ρ Free stream density
 ω Rotation rate, 0 to 350 rpm (36.65 rad/sec)

Model component/support designations:

B Body
W Wing
L LEX
H Horizontal tail
V Vertical tail
S Strake

BT	British transition strips (DRA)
IT	Italian transition strips (AerMacchi)
R	Rear entry sting support
T	Top entry sting support
EI	Eidetics International/NASA, USA
DRA	Defence Research Agency, UK
AM	AerMacchi, Italy
FFA	Aeronautical Res. Inst. of Sweden

Introduction

AGARD Working Group 16 was organized in 1991 as a result of recommendations (Ref. 1) by AGARD Working Group 11 on "Rotary-Balance Testing for Aircraft Dynamics" to establish a "Cooperative Program on Rotary Experiments for Maneuvering Aircraft Dynamics" to compare and correlate rotary-balance and forced-oscillation test data from many facilities and their respective rigs on a common configuration. The goals of these cooperative experiments are to provide comparison and evaluation of wind tunnel wall and model support interference effects, correlation of results between rotary balance and oscillatory rigs, evaluation of configuration build-up effects, understanding of the physics and effects of rotary flows on the forces and moments, to provide a comprehensive experimental data base for aerodynamic math modeling studies and for comparison to computational aerodynamic results focused on preliminary aircraft design methods.

To accomplish these goals, three models of the same configuration have been constructed and have been or will be tested on rotary-balance rigs in the United Kingdom, United States, Italy, Germany, France, and Sweden and on forced-oscillation rigs in Canada, U. K., Italy, Germany and France. The generic fighter configuration is shown in Fig. 1. Two of the models are identical in size (Model A) and one is smaller (Model B). Model B (dimensions are shown in Fig. 1) is 73% scale of Model A. This configuration is nearly identical to a generic fighter configuration referred to as the NASA Langley/Eidetics generic fighter configuration tested extensively by Eidetics International in the Langley 12-Foot Low Speed Wind Tunnel in 1987 as part of a research program on forebody vortex control (Refs. 2-7).

Model B, the first model to be tested, was constructed by DRA in the U.K. and tested in the DRA Bedford 13 x 9-Ft Wind Tunnel in October 1992. One of the purposes of the first test was to establish a common baseline configuration that every participant would be required to test (variations were optional but desirable). The principal issue for configuration selection was how to configure the forebody, i.e., whether to use strakes to force symmetric vortices at high angles of attack and whether to rely on natural transition or to grit the model appropriately to induce boundary-layer transition. DRA experimented with both a clean forebody (no strakes) and a forebody

with strakes (with and without grit). The "standard" configuration that was ultimately chosen as the common model has a forebody with transition grit strips at +/- 40° and strakes at +/- 105° from the windward stagnation line. (A brief description of the DRA experimental results for the grit/strake study is included later.) Reference 8 is a report on the results of the DRA tests.

Eidetics International next tested the B model in the Ames 7 x 10-ft wind tunnel, and the results are presented in Refs. 9 and 10. This model was then tested by AerMacchi in their 2-m low-speed tunnel and subsequently in the FFA 3.6m low-speed tunnel (LT1), with results reported, respectively, in Refs. 11 and 12. AerMacchi also tested the A model, as will ONERA and DLR.

Models

The B model, constructed by DRA, is made primarily of aluminum alloy and weighs approximately 17 pounds. The fuselage is of circular cross-section and all other components are flat plate sections with edges chamfered at a 40° included angle except the wing tips which have a 60° included angle. The model is constructed to allow a configuration buildup with body alone, body-wing, body-wing-LEX, and body-wing-LEX-horizontal-vertical tails. Two aft bodies are available, one with wings and one without. The horizontal tails are fixed at 0° deflection. The model can be mounted on either a rear-entry or top-entry sting. For the Eidetics/Ames tests the model was mounted only at the rear. For the DRA, AerMacchi and FFA tests, the model was mounted both in the rear and through the top.

As a result of the preliminary tests at DRA, the forebody has 0.2 mm grit strips 3 mm wide symmetrically disposed on the windward side at radial locations +/-40° from the x-z plane. The strips run between the tip of the nose and the LEX apex. The grit strips applied for the DRA tests were left in place for all of the Eidetics/Ames tests. The DRA grit strips were removed by AerMacchi in order to do some tests without grit and then grit was reapplied using their own technique consisting of strips in the same location as the DRA strips using a string of resin disks with a thickness of 0.2 mm, a diameter of approximately 1.5mm and a spacing of 2.5mm. The FFA tests were conducted at two different times and, therefore, test results exist with grit patterns from each of the DRA and AerMacchi applications. A rationale for selecting the final grit strips and some examples of data with and without them are provided later in the discussion of some of DRA's preliminary data. The forebody was also tested with and without nose strakes. The strakes are 1.0 fuselage diameter in length and 0.1d in height at the trailing edge. The strakes are attached normal to the forebody surface at radial angles of +/-105° (see Fig. 2).

The A model was designed, primarily, by IMFL in France, and various components were constructed in Italy by AerMacchi (fuselage), in Germany by DLR (aerodynamic surfaces) and in the UK by DRA (horizontal tail disks). The model is constructed mainly of aluminum alloy and PVC resin. Its components were assembled in Italy by the Politecnico di Torino. For the experiments discussed in this paper, the A model was used only by AerMacchi. (ONERA-IMFL and DLR are also using the A model for their rotary-apparatus tests, but the results are not yet available.)

Rotary-Balance Apparatuses

Defence Research Agency

The DRA apparatus is shown in Fig. 3. A five-component strain gage balance (no axial force) is machined on the end of the sting, which can be axially rotated in the sting carrier to vary sideslip angle. The 40° crank angle provides for angles of attack from -12° to 40°, the 60° crank provides for 8° to 60° and the 90° crank provides for 50° to 90°. The angle of attack can be changed in increments of 1°. The rotation rate can be varied up to 350 rpm. Speed is controlled with a feedback system using a tachometer to provide the rate feedback signal. The rig is statically balanced for each angle of attack setting by adding the appropriate weights to the end of the rotor. The balance signals are brought across the rotating interface with a slip ring unit.

Eidetics/Ames

The Eidetics/Ames rotary-balance apparatus is a remodeled rig developed originally at NASA-Ames and last used in 1984. It is driven by a hydraulic pump and motor system with a tachometer used as feedback to a servo-valve for speed control. New hardware to support the model was recently designed by Eidetics International and constructed for tests with an F/A-18 model to investigate forebody vortex control techniques under rotating conditions. The same hardware was used for this test. The maximum rotation speed for the new hardware is 350 rpm. Figure 4 shows a drawing of the new apparatus hardware which includes a C-strut, strut arm and sting. The angle of attack is adjusted with discrete positions of the sting/clevis on the C-strut (0 to 60° in 3° increments), and sideslip angle can be set by rolling the sting in the strut arm. The balance signals are brought across the rotating interface by cables running through a hollow motor drive shaft and a 50-channel slip ring unit mounted near the rear of the motor. For each discrete angle of attack setting, the rig is statically balanced by adding or subtracting weights on the end of the C-strut. Figure 4b shows a drawing of the special wind tunnel A-frame support structure and the rotary rig as it was installed in the 7x10-ft wind tunnel test section.

AerMacchi

The AerMacchi rig is shown in Fig. 5 as it appears in their 2-m low-speed tunnel which can be run either with an open test section (as illustrated) or as a closed test section. The body of the balance is supported on the tunnel axis by three swept struts attached to the tunnel diffuser. This body contains bearings for the rotating arm which is driven by an asynchronous motor via a variable-speed drive, two cardanic joints and a bevel gear pair. A clutch is also available. The body also contains a slip ring assembly which carries power supplies and carries out signals from the balance or other transducers. Angles of attack and sideslip from -180° to +180° can be set manually with different model mounts through the base, top or bottom of a typical model. The tunnel is capable of speeds up to 60 m/s. The rig can rotate up to 300 rpm.

Aeronautical Research Institute of Sweden (FFA)

The FFA rig is shown in Fig. 6 as used in their 3.6 m low speed tunnel (LT1), an atmospheric closed circuit tunnel with a maximum speed of 85 m/s. The rotary balance rig is driven by a hydraulic motor/pump. An electrical motor is used to set the angle of attack remotely. Angles of attack up to 150° can be set by using different sting mountings, a rear entry for 0 to 40° and two different top entries for 30° to 70° and 60° to 100°. Angles of attack outside this range can be achieved by yawing and rotating the model 180°. The rotation speed can be varied from 15 rpm to 360 rpm. Balance signals are carried out by a slip ring unit.

Test Conditions

Defence Research Agency

The tests were conducted with the B model in the DRA Bedford 13 x 9-ft tunnel. The nominal wind speed was 60 m/s (200 ft/s) with a consequent Reynolds number of 0.95×10^6 (based on wing mean aerodynamic chord) and rotation rates were varied from 20 rpm to 350 rpm. A few runs were made at 30 m/s or Reynolds number of 0.474×10^6 .

Eidetics/Ames

The DRA B model was tested in the Ames 7 x 10-ft low speed wind tunnel. Most of the model configurations were tested at three different free stream velocities, 200 ft/sec (60 m/s), 150 ft/sec (45 m/s), and 100 ft/sec (30 m/s) in order to assess Reynolds number effects. The corresponding Reynolds numbers are 0.955, 0.720, and 0.478×10^6 based on wing mean aerodynamic chord of 0.758 ft, or, based on fuselage diameter of 0.239 ft, the Reynolds numbers are 0.302, 0.226, and 0.151×10^6 . All of the various configurations from body alone to full

configuration were tested at angles of attack of 24°, 39°, and 51° and only the full configuration at 60°. These angles were chosen to compare to the DRA data as closely as possible (because of the 3° spacing on the C-strut, 40° and 50° could not be matched exactly, thus 39° and 51°). Some of the configurations, primarily those without strakes, were tested only at the high and low Reynolds numbers.

AerMacchi

Both Models A and B were tested by AerMacchi in their 20-m low-speed tunnel, and both were tested with the tunnel configured with an open and a closed test section. The majority of the tests were performed with the A model at a tunnel speed of 44 m/s resulting in a Reynolds number matching the previous tests in the DRA and Ames tunnels of 0.955×10^6 based on mean aerodynamic chord. The B model was run at 60 m/s with a few runs at 30 m/s. All of the rotary-balance tests were performed with the complete model with and without strakes. A few static runs were made with a B model configuration buildup.

Aeronautical Research Institute of Sweden (FFA)

The FFA tests were conducted in the 3.6m low-speed tunnel (LT1) with the B model on two different occasions, once with the transition strips as applied by DRA and once, later, with the strips as applied by AerMacchi. The tunnel speed was primarily at 60 m/s with a few runs at 30 m/s resulting in Reynolds number based on mean aerodynamic chord of 0.95 and 0.475×10^6 , respectively. The angle of attack ranged from 0 to 60°. Complete model as well as configuration buildup tests were run with and without forebody strakes.

Initial DRA Test Results

The tests performed in the DRA-Bedford 13 x 9-ft tunnel used the B model on the rig illustrated in Fig. 3. The model could be mounted through the base for angles of attack up to 60° and through the top for angles of attack from 50° to 100°. The initial tests investigated the effects of transition grit and strakes on the forebody. Figures 7 and 8 show these results. Figure 7 shows yawing moment data for the body alone with no strakes attached to the forebody. The effects of transition grit in two radial locations illustrates the sensitivity of the forebody flow to small changes on the forebody. Figure 8 shows data for the body alone at 40° AOA with strakes on and off with grit and with strakes on without grit. Somewhat surprisingly, the forebody with strakes was also sensitive to the effects of grit strips. Apparently, even though the forebody flow is forced to separate at the strakes, the resulting side forces and yawing moments are dependent on the condition of the boundary layer on the body aft of

the strakes. Tripping the boundary layer along the entire forebody appears to make the flow more stable.

In Fig. 9, the effect of strakes on the configuration with body-wing-LEX is also evident, with the strake configuration showing significantly less asymmetry in yawing moment and side force. Based on these results, it was decided that the "baseline" forebody configuration should have transition strips at +/-40° and strakes. The majority of the DRA runs were made with this configuration, and all of the Ames tests were conducted with the same grit strips at +/- 40° as the DRA tests (i.e., the grit strips applied by DRA for their tests were left in place for the Ames tests). The first set of FFA tests also used the DRA grit strips. AerMacchi tested the model without grit strips and then with their own grit strip application. The second set of FFA tests (following the AerMacchi tests) used the AerMacchi strips. In the discussion of results, the DRA and AerMacchi grit strips are designated on the plots with BT (British transition strips) and IT (Italian transition strips). The only facility where both were tested is FFA in Sweden.

Discussion of Results

As discussed above, the early tests by DRA with and without transition and forebody strakes resulted in a consensus among the experimenters that the "standard" configuration should have transition strips and forebody strakes, and comparisons between facilities would be made primarily with this configuration. However, each of the experimenters also conducted tests on the model without forebody strakes and, while, direct comparisons of only these experimental results could be misleading, there are some interesting data that are worth presenting and discussing. Figures 10 through 13 will show some of the results for tests without forebody strakes and the remainder of the results, Figures 14 through 21 will be devoted to comparisons of data for the configuration with forebody strakes. Also, although all six force and moment coefficients were measured, this paper will focus on side force, yawing moment, and rolling moment coefficients.

(A) Model without forebody strakes

(A1) Effects of Reynolds number, with and (without) forebody strakes

Figure 10 shows a comparison of EI/Ames results with the B model for the body-wing-LEX configuration at 40° AOA with different Reynolds numbers (values shown are based on wing mean aerodynamic chord), one set without forebody strakes and one with forebody strakes. There is a larger effect of Reynolds number for the strake-off configuration than the strake-on configuration. For the strake-off model, the lower Reynolds number data also

show a larger asymmetry in side force and yawing moment at zero rotation rate than for the higher Reynolds number data. It is interesting, though, that the reversal in sign (likely caused by reversal in orientation of the forebody vortices) of the yawing moment and side force at the maximum negative rotation rates is evident at both Reynolds numbers. The rolling moment coefficients do not differ as much as the yawing moment with Reynolds number. In fact, there is more difference due to strakes on an off. The data with forebody strakes at both Reynolds numbers are in closer agreement than for the model with strakes-off.

(A2) Effects of model support and test facility/rig. without forebody strakes

Figure 11 shows an example of the sensitivity of the aerodynamics for the body-wing-LEX (BWL) configuration (B model) without forebody strakes at 40° AOA to a change in the model support geometry. The two curves from DRA tests with two different crank angles (See Fig. 3) are substantially different, illustrating that the forebody vortices have a tendency to be bistable at this angle of attack, i. e., the asymmetry can either be with the right vortex above the left or vice versa with resulting side force and yawing moment coefficients being either positive or negative. As has been seen in many static tests in the past, asymmetry orientation can be reversed by very minor disturbances in the flow field, either on the forebody itself or by disturbances downstream of the model. The third curve is from the Eidetics/Ames tests for the same configuration with, obviously, a different model support scheme (See Fig. 4). What is remarkable is the similarity between the EI curve and the DRA curve for the 40° crank, particularly the jump at the maximum negative rotation rates. An important point to made with this figure, and one of the reasons for including it, is to illustrate that there may be wide differences between results on the same model (if the flow field is very sensitive to disturbances of almost any origin) in the same facility with only a change in the way the model is mounted, and, yet there can be remarkable similarities between data acquired in different facilities and with completely different test rigs. One simply has to be very careful about drawing conclusions about the reasons for the significant changes in the aerodynamics.

(A3) Effects of model size. without forebody strakes

Figure 12 shows one example of testing the same configuration (BWLHV) at 40° AOA, but with two different size models in the same closed test section. AerMacchi tested both the A and B models in their facility. This figure shows the differences observed for the model without strakes. Later, a comparison is made for the models with strakes. There is a substantial difference, again illustrating the high sensitivity of the

flow field and resulting forces and moments to subtle differences which will exist by necessity with two different scale models of the same configuration (at the same model Reynolds number). The differences could be caused by either a model difference or by the fact that the larger model (Model A) may have more influence from the tunnel walls or blockage than the smaller model (Model B). With these data alone, there is no way to separate the effects. Eliminating the sensitivity of the sharp nose with strakes, as shown later, helps to sort out the principal cause for the differences.

(A4) Effects of open and closed test section. without forebody strakes

Figure 13 is an example of a comparison for tests on the complete Model B at 40° AOA in the AerMacchi wind tunnel with and without tunnel walls in place. The "open" test section runs are actually one run. Run 25721 is acquired with the rotation beginning at the maximum negative value and ending at the maximum positive value (as are all of the other runs, the usual order in which the rotary-balance data are taken). Run 25722 is a continuation of this run with the rotation rate progressing from maximum positive to maximum negative. The immediate observation is the hysteresis that occurs in the region of $\omega b/2V = -0.05$. This is not so unusual for configurations such as this with sharp forebodies and vortex asymmetries that tend to be bistable. The orientation of the left and right vortices are dependent not only on the local flow angle of the velocity vector with respect to the nose but also on the history or path to reach that flow angle, as it varies with either sideslip angle, for example, or, on a rotary rig, with rotation rate and rotation direction. The abrupt change in the side force and yawing moment in Fig. 13 indicates the reversal in the orientation of the forebody vortices once a certain local forebody flow condition is reached. The data from the closed test section test also shows the "jump" from one asymmetric condition to the opposite occurring at $\omega b/2V = 0.02$. The point at which the jump occurs depends, obviously, on the condition of the test section, i. e., wall interference, blockage, etc. This sensitivity is greatly reduced for a model with forebody strakes, as will be shown later.

Summary of results without forebody strakes

The principal objective of these cooperative experiments was to evaluate the effects of sting mounting arrangements, tunnel blockage and wall interference effects (open vs closed test section), Reynolds number, etc., on a model that is not overly sensitive to minor disturbances, as can be the case for a pointed ogive forebody. However, it is also possible that the flow field can be too stabilized at high angles of attack by fixing separation at sharp edges on all the components (forebody included if strakes are installed) that the

sensitivity is reduced to the point where the flow field differences caused by the principal parameters listed above are minimal and the conclusion will be that some or all of these parameters are unimportant. The degree to which they are important will obviously depend on the type of configuration being tested. If the configuration has a sharp forebody, as most current fighters do, knowledge of the parameters that have the most influence on the measured aerodynamic forces and moments will be even more important than for those configurations that have quite stable flow fields. It will be important to consider not only the data with forebody strakes, but also data without forebody strakes. The next section discusses results acquired on models with forebody strakes, and comparisons between facilities etc. will be included.

(B) Model with forebody strakes

(B1) Effects of Reynolds number, sting mounting and facility

Figure 14 shows data for the body-wing-strakes (BWS) configuration (Model B) at 40° AOA from three facilities, each with a different mounting arrangement and at two different Reynolds numbers. The lower Reynolds number data obtained by EI and FFA agree quite well, particularly side force and yawing moment, and are both somewhat different than the higher Reynolds number results. The rolling moment results show minor differences among all of the runs. The high Reynolds number data also correlate quite well from all three facilities. In contrast to the large nonlinearities observed for the configuration without forebody strakes, the curves shown here are very well-behaved with rotation rate and are nearly linear. It should be pointed out that the FFA results were acquired with a top-mounted model, while the EI and DRA results were obtained with a rear mounted model. There appears to be little or no effect of sting mounting differences.

(B2) Effects of different transition strips and Reynolds number

Another interesting comparison is the dependency of the results on the application of grit. In Fig. 15, there are plots for data with the body-wing-strake (BWS) configuration at 40° AOA at the same Reynolds number, one for a rear-mounted model and the British/DRA grit application (BT) and two (one with rear mount and one with top mount) with the Italian/AerMacchi grit application (IT). There are no discernible differences in these results except for the small difference between the low and high Reynolds number data. There is no significant difference between results with top and rear-mounted models at the same Reynolds number, regardless of the grit applications.

(B3) Effects of Reynolds number and model/sting mounting

Figure 16 shows an example of Reynolds number comparisons and different sting mounting arrangements for the body-wing-LEX configuration at 40° AOA. The EI data are obtained with a rear-mounted model and the FFA data with a top-mounted model. There are some small differences between the two sets of EI data at the two Reynolds numbers as observed earlier in Fig. 10. The lower Reynolds number FFA data, however seem to agree better with the high Reynolds number data for EI. The difference in these two curves are most likely caused by the different mounting arrangements and different facilities. It should also be noted that the DRA data also agree quite well with the data from the other facilities. As noted previously, the strakes minimize the sensitivity of the aerodynamic forces and moments to Reynolds number and sting arrangements by stabilizing the forebody vortices and forcing separation at the forebody strake edges.

(B4) Effects of facility, model size and model/sting support options

Figure 17 shows examples of data on the complete configuration (BWLHVS) in four different facilities with Models B and A at 24° AOA. Despite being acquired in four facilities, with different size models and different sting arrangements, the data are in near perfect agreement. Figure 18 shows a similar comparison at 40° AOA and there is a little more disagreement between various test results. Overall, the data all agree quite well with the only exception being the DRA data with the 40° crank angle. The DRA data with 60° crank angle agree much better with the other results.

Figure 19 shows a similar type of comparison as in Fig. 18, except the angle of attack is 50° rather than 40°. Also, the DRA data are for 60° and 90° crank angles and the FFA data are acquired with a top-mounted rather than rear-mounted model. Despite all of the different combinations of facility, model size and sting support arrangement, the data all match each other almost perfectly.

(B5) Effects of open versus closed test section

Figure 20 shows an example of data acquired by AerMacchi on the A model with test section walls in place and with them removed. Based on the plotted curves, there are few, if any, differences that stand out simply because of tunnel wall effects. These data were all acquired by Model A. Figure 21 shows the same comparison as Fig. 20, but with the B model instead. There are some very small differences between the data from open and closed test sections, but not much.

Conclusions

As part of an AGARD working group research program, two different size models of a generic fighter configuration have been tested on rotary-balance apparatuses in four different facilities in the U. K. (DRA), U. S. (Eidetics/Ames), Italy (AerMacchi) and Sweden (FFA). The low-speed wind tunnels are all different sizes, three with closed test sections and one with the option of either closed or open. The rotary rigs are similar in geometry but yet quite different in detail and size. The models were tested with transition strips on the forebody and with and without forebody strakes. A limited number of tests were run at different Reynolds numbers.

Overall, the differences between the results in various facilities and rigs were very sensitive to whether the model had strakes on the forebody or not. Without forebody strakes, the forebody vortices are easily influenced by variations in Reynolds number, sting geometry and attachment schemes, model size differences and tunnel wall effects. With forebody strakes, there was relatively good agreement between all of the test results compared.

With completion of the remaining rotary-balance tests at ONERA-IMFI in France and DLR in Germany, along with the data described here, there will be a very substantial rotary-balance data base from six different facilities for complete analysis. By systematically comparing data from all of these facilities, for complete configurations as well as buildup configurations, with and without forebody strakes, with rear-mounted and top-mounted models, with models of different sizes and with test sections both open and closed, it is expected that a great deal will be learned about the relative importance of all of these parameters for future rotary-balance testing. Progress to date in this ambitious cooperative research program is reflected in the sample of results discussed in this paper. Ultimately, an AGARD Working Group 16 report will be published, providing a thorough analysis of all of the experimental results.

References

- 1) "Rotary-Balance Testing for Aircraft Dynamics", AGARD Advisory Report No. 265, Report of the AGARD Fluid Dynamics Panel Working Group 11, December 1990.
- 2) Malcolm, G.N., "Forebody Vortex Control," Special Course on Aircraft Dynamics at High Angles of Attack: Experiments and Modeling," presented at NASA Langley Research Center April 8-11, 1991 and von Karman Institute April 22-25, 1991, AGARD Report No. 776, March 1991.
- 3) Malcolm, G.N., "Forebody Vortex Control," Progress in Aerospace Sciences, Vol. 28, pp. 171-234, 1991.
- 4) Malcolm, G.N., Ng, T.T., Lewis, L.C. and Murri, D.G., "Development of Non-Conventional Control Methods for High Angle of Attack Flight Using Vortex Manipulation," AIAA Paper 89-2192.
- 5) Malcolm, G.N., Ng, T.T., "Forebody Vortex Manipulation for Aerodynamic Control of Aircraft at High Angles of Attack," SAE Paper 892220.
- 6) Malcolm, G.N., Ng, T.T., Lewis, L.C. and Murri, D.G., "Development of Non-Conventional Control Methods for High Angle of Attack Flight Using Vortex Manipulation," AGARD CP 465, Paper No. 11, April 1990.
- 7) Malcolm, G.N. and Ng, T.T., "Aerodynamic Control of Fighter Aircraft by Manipulation of Forebody Vortices," AGARD CP-497, Paper No. 15, November 1991.
- 8) O'Leary, C.O., Wier, B. and Walker, J.M., "Continuous Rotation Tests of a Generic Combat Aircraft Model in a Low Speed Wind Tunnel", DRA Tech Memo AERO/PROP 42, 1993.
- 9) Malcolm, G.N., Kramer, B.R., Suárez, C.J., Ayers, B.F. and James, K.D., "Rotary-Balance Tests in NASA-Ames 7 x 10-Ft Wind Tunnel with AGARD Generic Fighter Model", EI TR 93-004, March 1993.
- 10) Malcolm, G.N., Kramer, B.R., Suarez, C.J., James, K.D., O'Leary, C.O., Wier, B. and Walker, J. M., "US/UK Rotary-Balance Test Comparisons with a Generic Fighter Model", AIAA Paper 94-0196.
- 11) Visintini, L. - Private communication from AerMacchi with data from preliminary wind tunnel data report, March 1994.
- 12) Rafatnia, Farshad, "Rotary-Balance Tests with AGARD Generic Fighter Model in FFA Low Speed Wind Tunnel LT1," FFA-TN-1994-15, March, 1994.

Dimensions in mm (inches) unless noted

All chamfers 40° Included angles except wing tip which is 60°

Thickness of wings, LEX, tails = 10 mm (0.394 in.)

$S = 0.1032 \text{ m}^2$ (1.1109 ft²)

$B = 0.5009 \text{ m}$ (1.643 ft)

$\bar{c} = 0.2313 \text{ m}$ (0.758 ft)

AR = 2.43

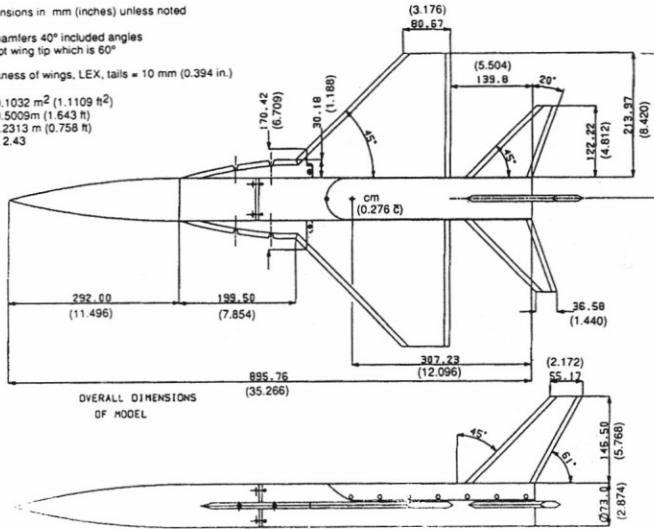


Figure 1 - AGARD FDP Model WG16B

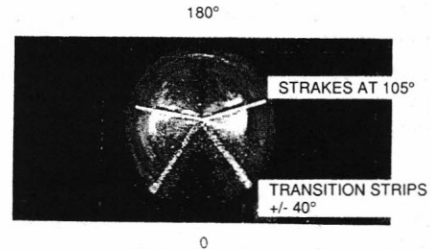
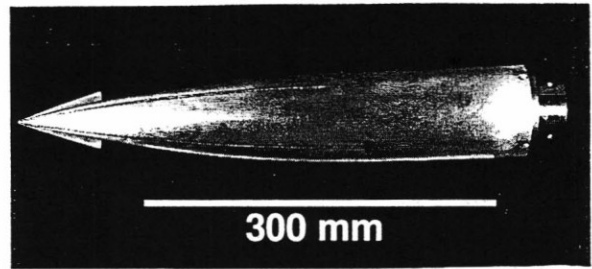


Figure 2 - Forebody strakes and grit locations

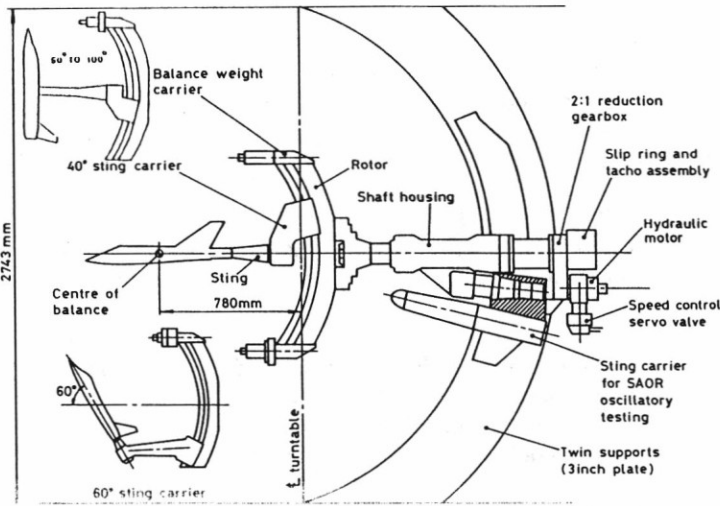


Figure 3 - DRA-Bedford rotary apparatus in 4.0x2.7m (13x9-ft) wind tunnel

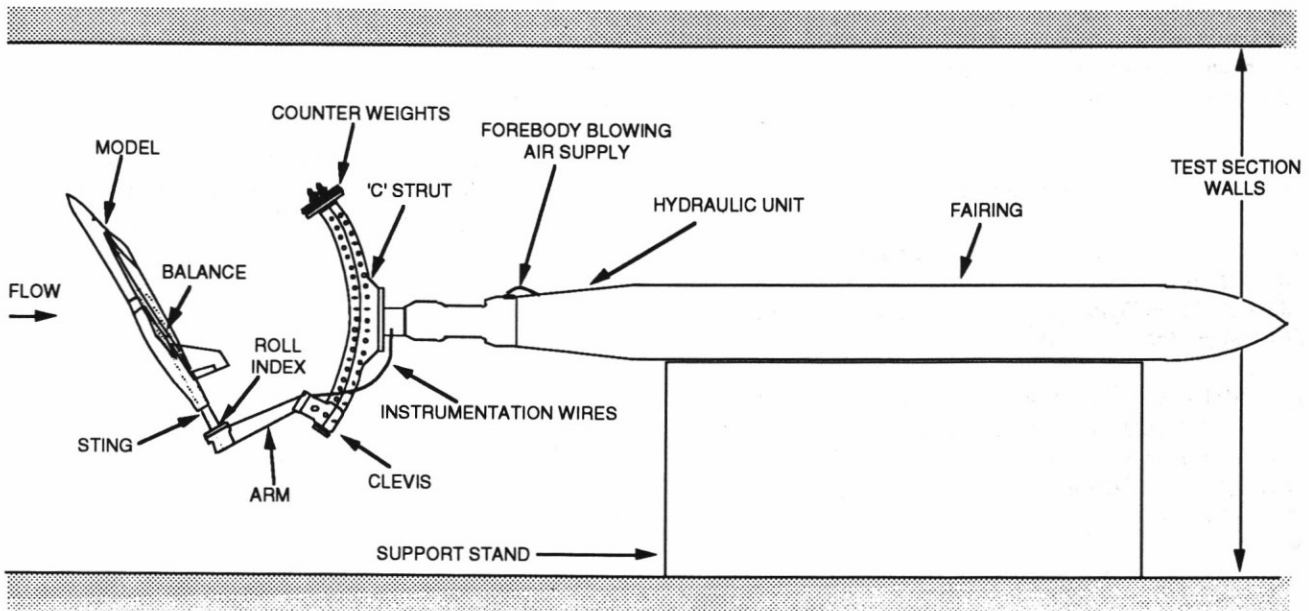


Figure 4 - New NASA Ames rotary-rig hardware and support system in Ames 7 x10-ft wind tunnel

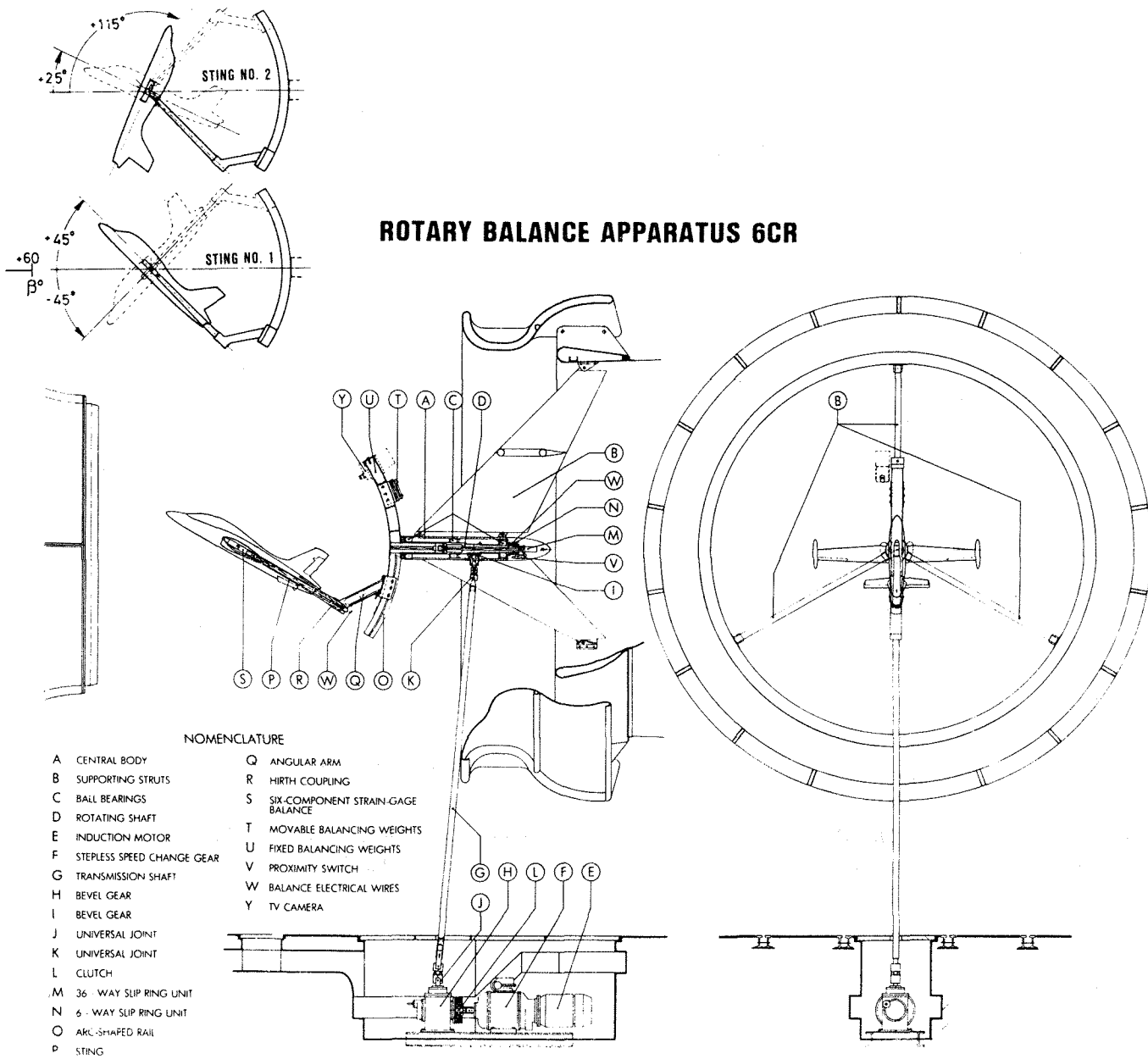


Figure 5 - AerMacchi Rotary-Balance Rig

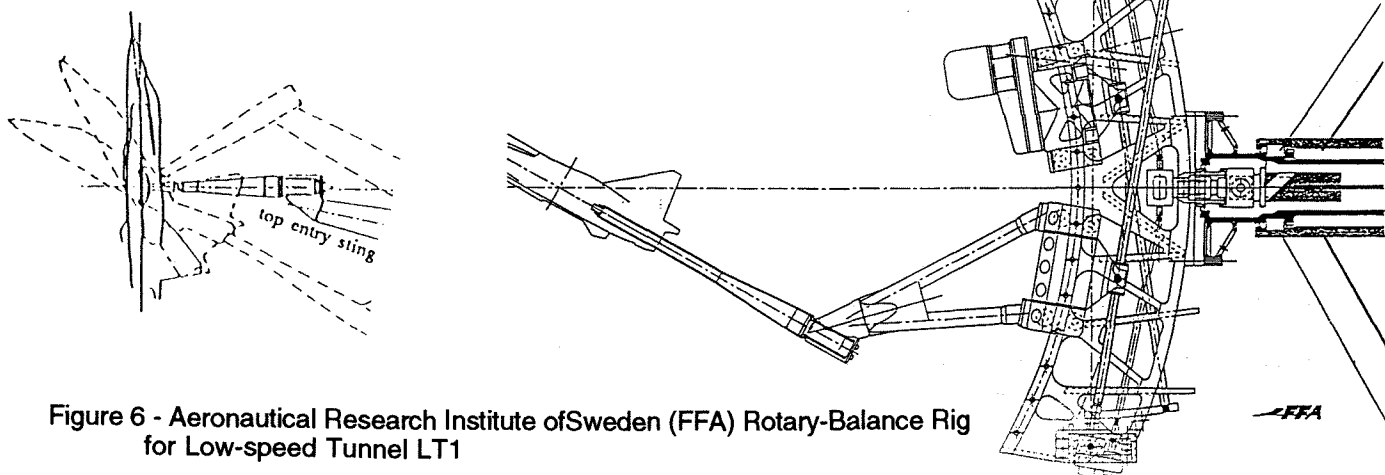


Figure 6 - Aeronautical Research Institute of Sweden (FFA) Rotary-Balance Rig for Low-speed Tunnel LT1

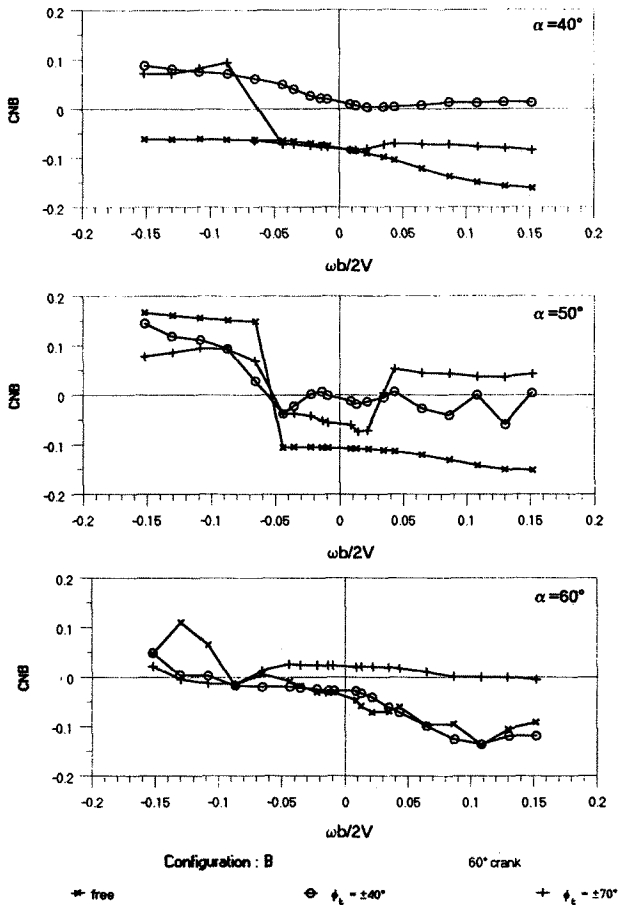


Figure 7 - Effects of transition strips, forebody alone, $R=0.955 \times 10^6$ (Ref. 8)

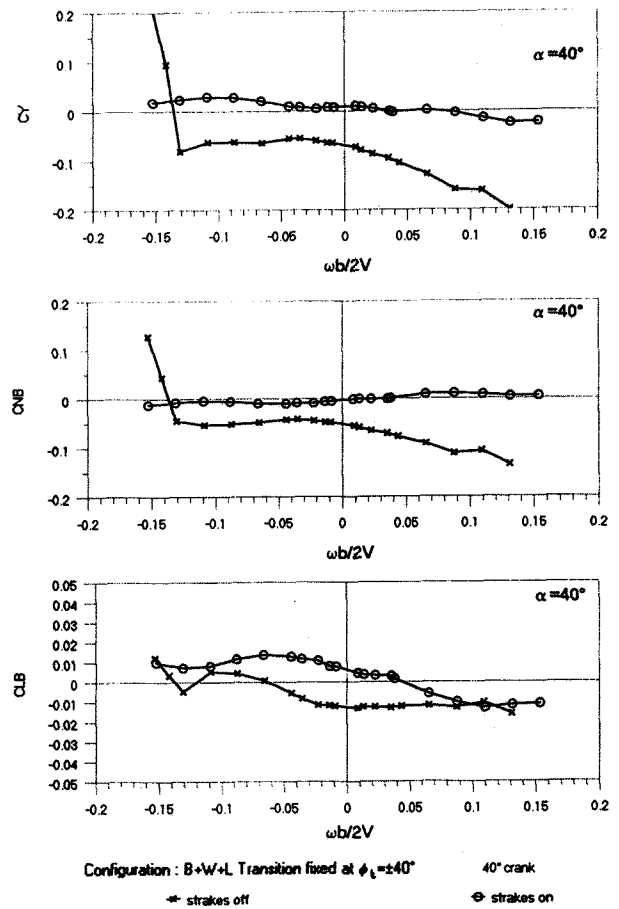


Figure 9 - Effects of nose strakes for BWL, $R=0.955 \times 10^6$ (Ref. 8)

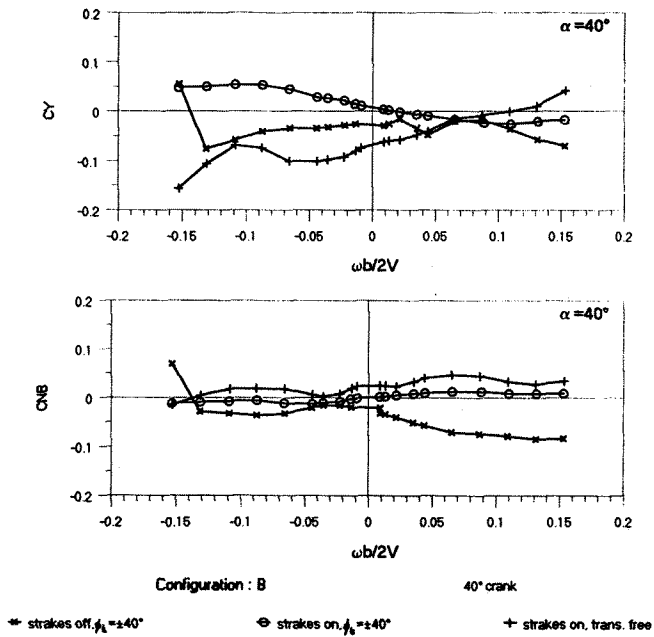


Figure 8 - Effects of nose strakes, forebody alone, $R=0.955 \times 10^6$ (Ref. 8)

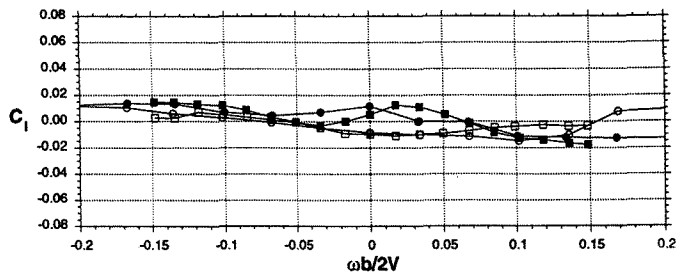
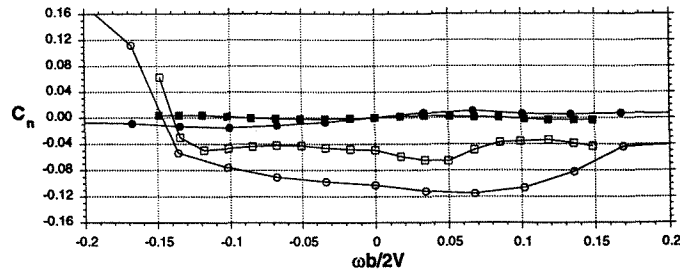
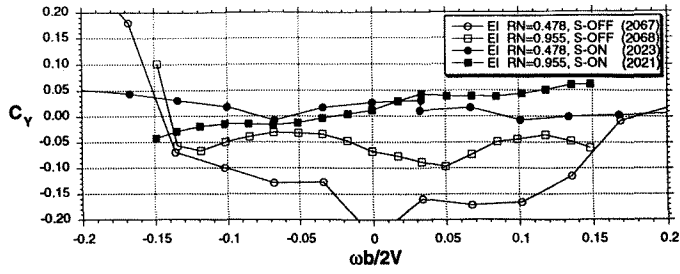


Figure 10 - Effects of Reynolds no., BWL, with/without strakes, 40° AOA

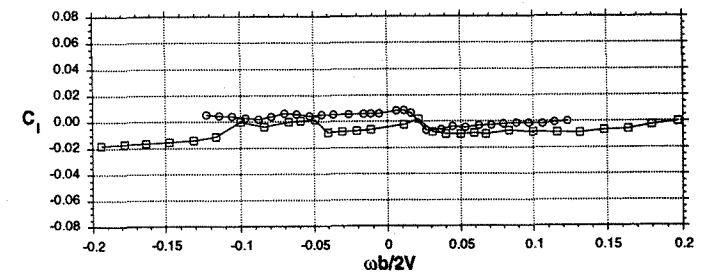
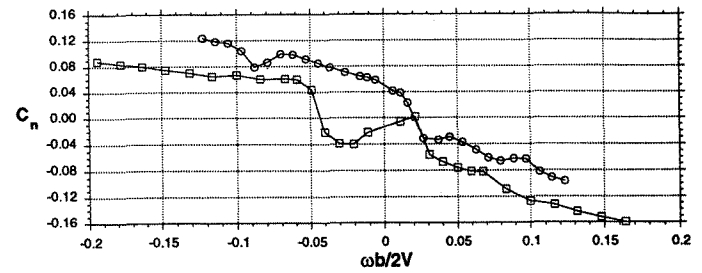
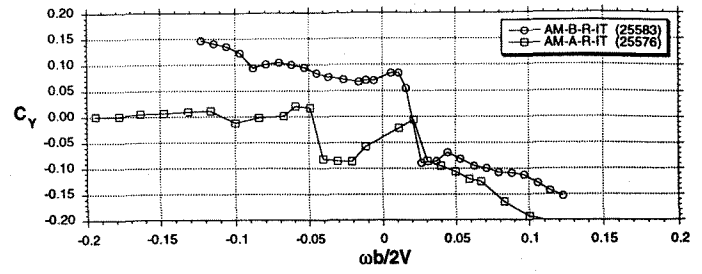


Figure 12 - Effects of model size, BWLHV, 40° AOA, R=0.955x10⁶

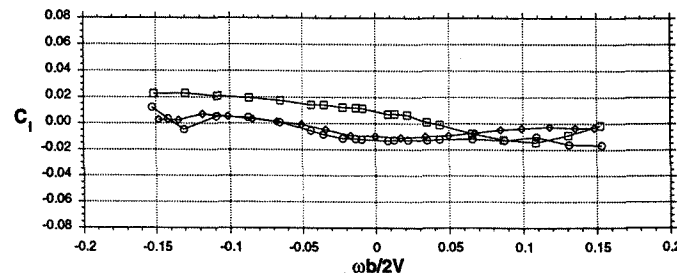
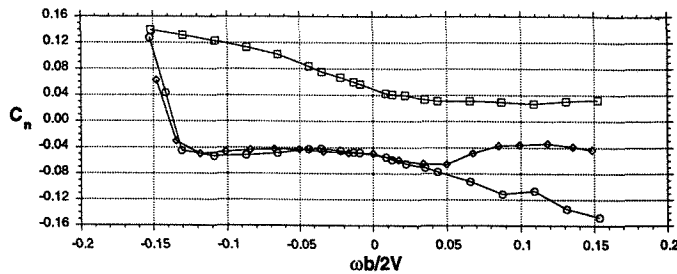
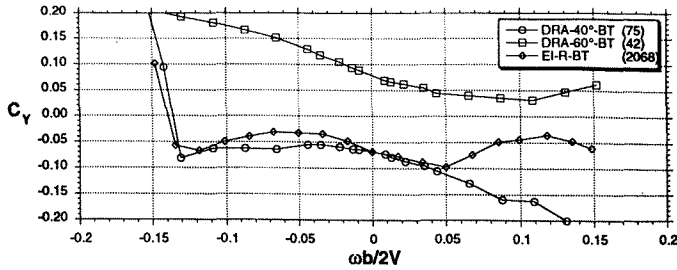


Figure 11 - Effects of model support and test facility, BWL, 40° AOA, R=0.955x10⁶

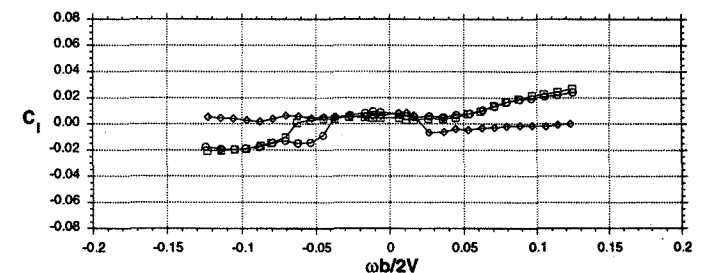
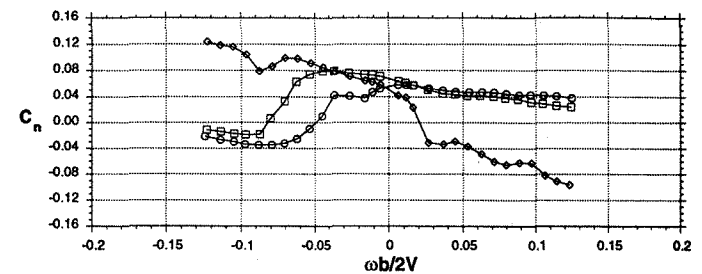
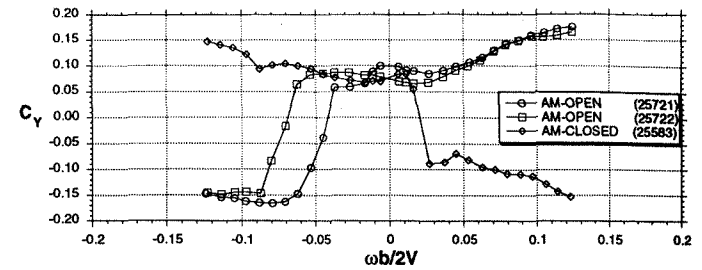


Figure 13 - Effects of open/closed test section, Model B, BWLHV, 40° AOA, R=0.955x10⁶

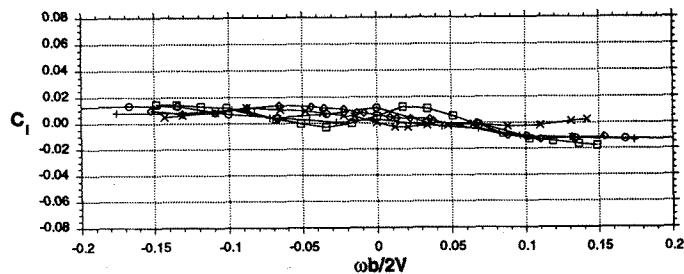
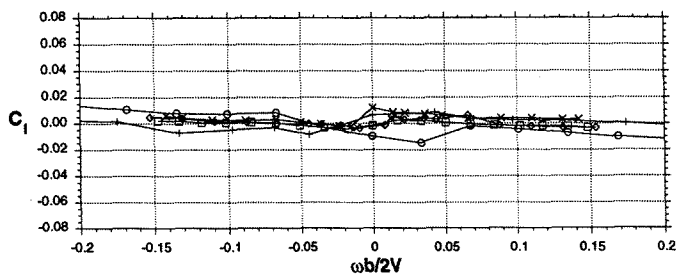
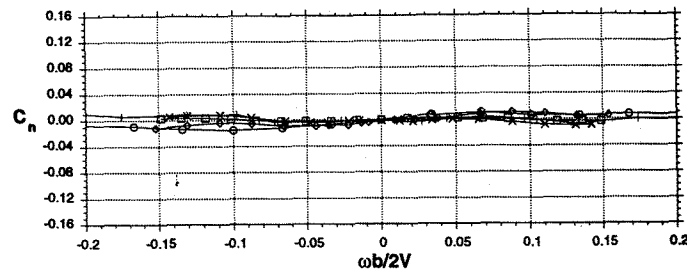
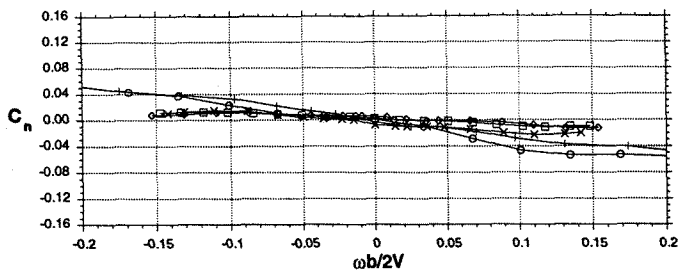
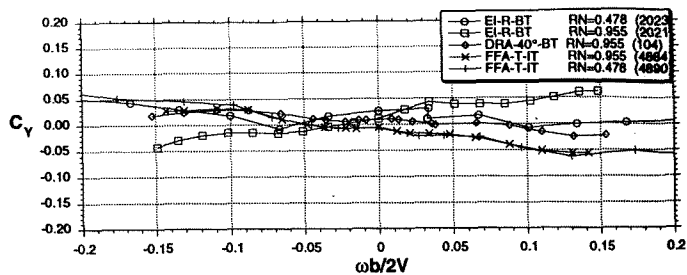
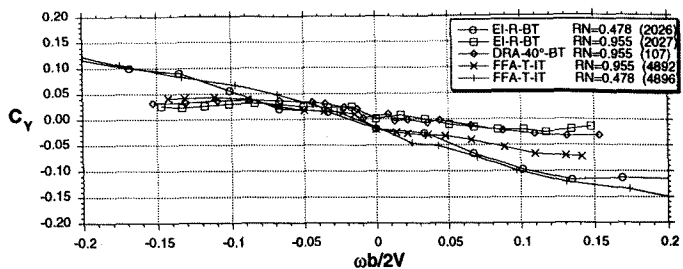


Figure 14 - Effects of Reynolds no., sting mount and facility, Model B, BWS, 40° AOA

Figure 16 - Effects of Reynolds no., sting mount and facility, BWLS, 40° AOA

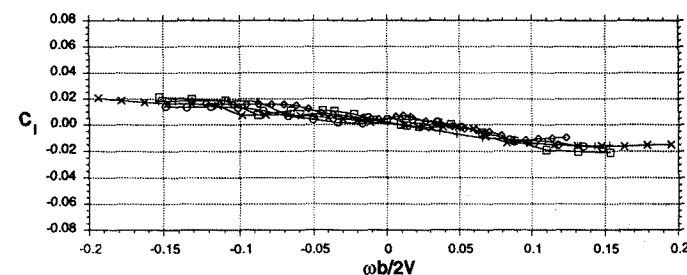
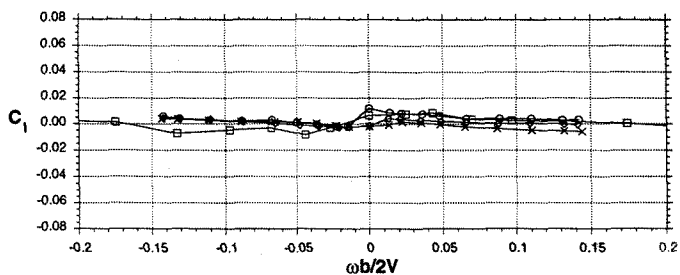
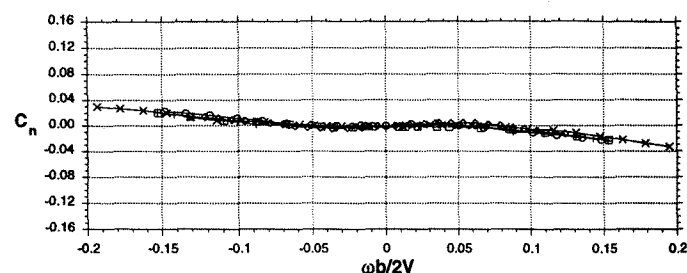
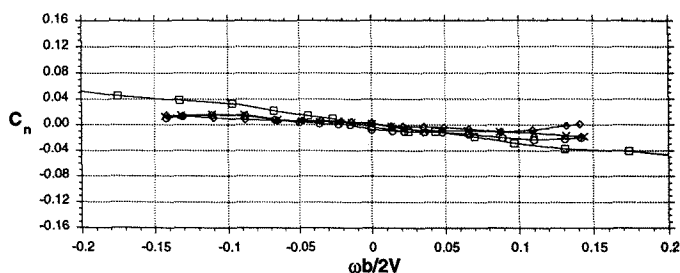
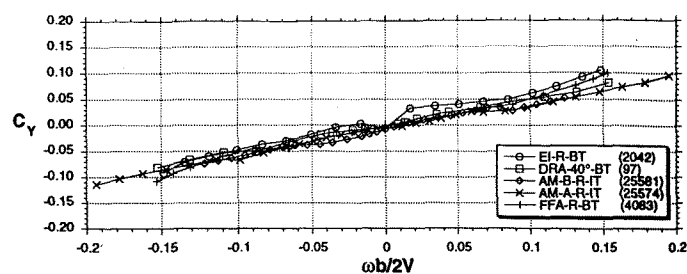
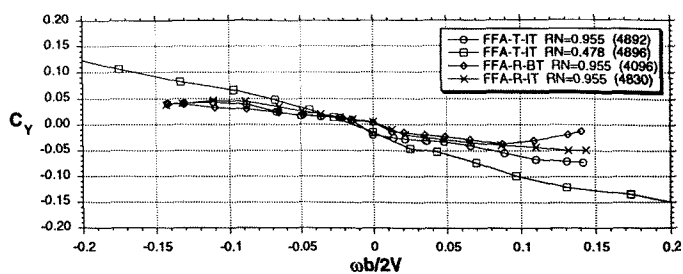


Figure 15 - Effects of transition strips and Reynolds no., Model B, BWS, 40° AOA

Figure 17 - Effects of facility, model size, sting mount, BWLHVS, 24° AOA, $R=0.955 \times 10^6$

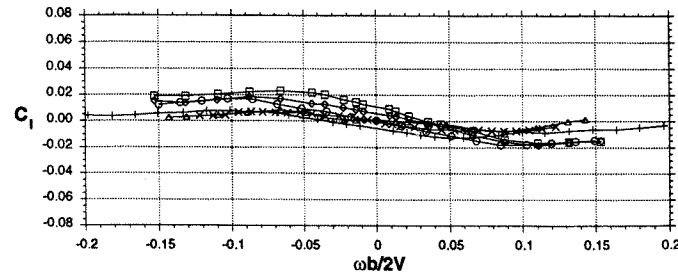
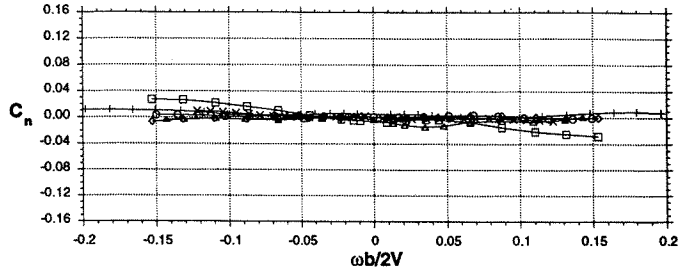
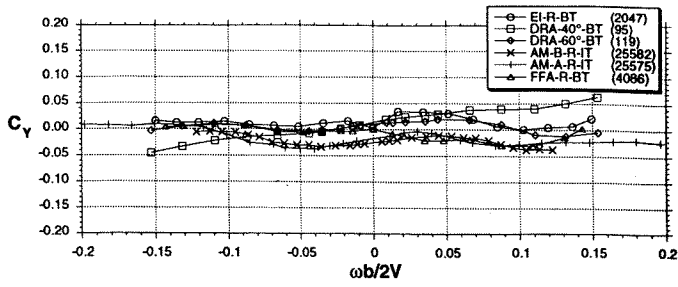


Figure 18 - Effects of facility, model size and sting mount, BWLHVS, 40° AOA, $R=0.955 \times 10^6$

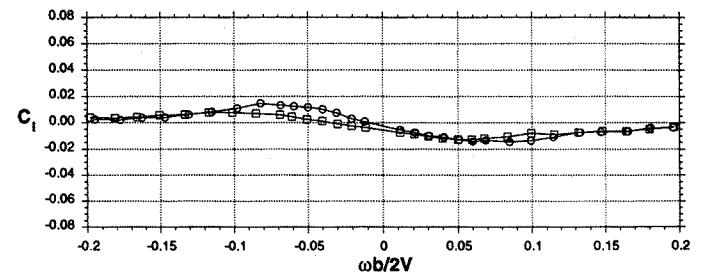
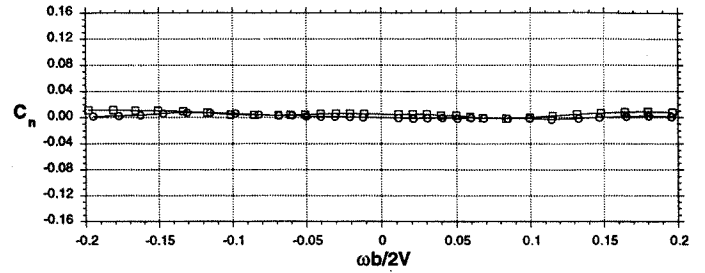
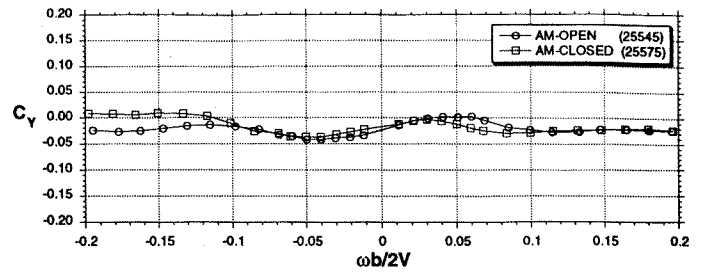


Figure 20 - Effects of open vs closed test section, Model A, BWLHVS, 40° AOA, $R=0.955 \times 10^6$

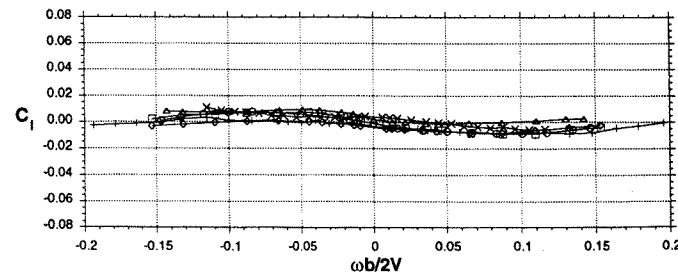
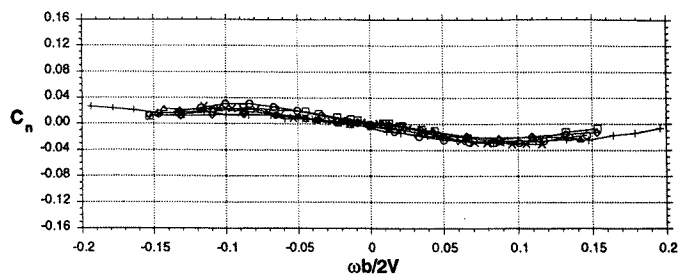
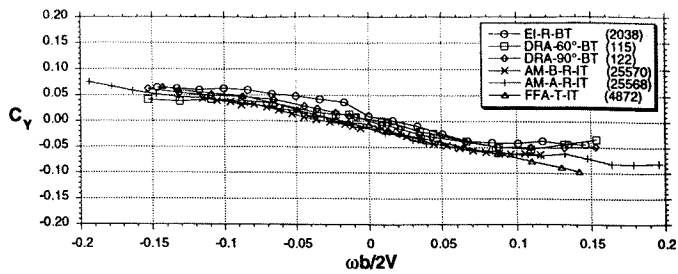


Figure 19 - Effects of facility, model size and sting mount, BWLHVS, 50° AOA, $R=0.955 \times 10^6$

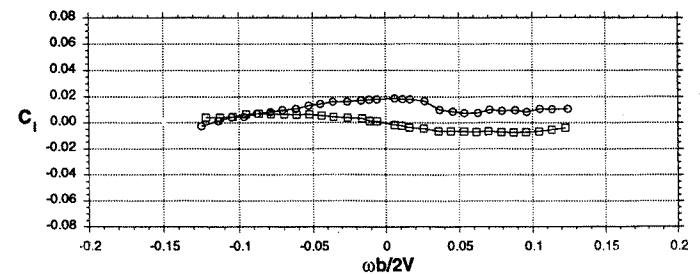
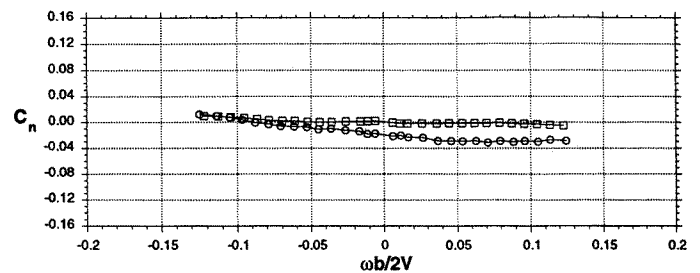
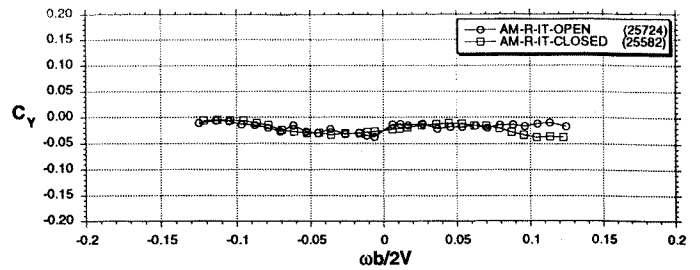


Figure 21 - Effects of open vs closed test section, Model B, BWLHVS, 40° AOA, $R=0.955 \times 10^6$